

RESEARCH ARTICLE

Modelling tree stem-water dynamics over an Amazonian rainforest

Binyan Yan¹ | Jiafu Mao²  | Robert E. Dickinson¹ | Peter E. Thornton² | Xiaoying Shi² | Daniel M. Ricciuto² | Jeffrey M. Warren² | Forrest M. Hoffman³

¹Jackson School of Geosciences, the University of Texas at Austin, Austin, TX

²Environmental Sciences Division and Climate Change Science Institute, Oak Ridge National Laboratory, Oak Ridge, TN

³Computational Sciences and Engineering Division and Climate Change Science Institute, Oak Ridge National Laboratory, Oak Ridge, TN

Correspondence

Binyan Yan, Jackson School of Geosciences, the University of Texas at Austin, Austin, TX 78712.

Email: byan@utexas.edu

Jiafu Mao, Environmental Sciences Division and Climate Change Science Institute, Oak Ridge National Laboratory, Oak Ridge, TN 37831-6301.

Email: maoj@ornl.gov

Funding information

Oak Ridge National Laboratory, Grant/Award Number: DE-AC05-00OR22725

Abstract

A novel tree stem-water model was developed to capture the dynamics of stem-water storage and its contribution to daily transpiration. The module was incorporated into the Community Land Model (CLM), where it was used to test model sensitivity to stem-water content for an evergreen rainforest site in Amazonia, that is, the BR-Sa3 eddy covariance site. With the inclusion of the stem-water storage, CLM produced greater dry-season latent heat flux that was closer to observations, facilitated by easier canopy access to a nearby stem-water source, rather than solely dependent on soil water. The simulated stem-water content also showed seasonal variations in magnitude, along with the seasonal variations in sap flow rate. Stored stem-water of a single mature tree was estimated to contribute 20–80 kg/day of water to transpiration during the wet season and 90–110 kg/day during the dry season, thereby partially replacing soil water and maintaining plant transpiration during the dry season. Diurnally, stem-water content declined as water was extracted for transpiration in the morning and then was refilled from soil water beginning in the afternoon and through the night. The dynamic discharge and recharge of stem storage was also shown to be regulated by multiple environmental drivers. Our study indicates that the inclusion of stem capacitance in CLM significantly improves model simulations of dry-season water and heat fluxes, in terms of both magnitude and timing.

KEYWORDS

Amazonian rainforest, Community Land Model, drought, tree stem-water model

1 | INTRODUCTION

The internal water storage inside tree stems has been recognized to play key roles in regulating water economy and in functioning of trees on time scales ranging from diurnal to seasonal, by maintaining daily transpiration (e.g., Goldstein et al., 1998), controlling stomata opening

(Meinzer, 2002), buffering drought impacts (e.g., Huang et al., 2017), and supporting leaf growth in the dry season for seasonally deciduous trees (Chapotin et al., 2006). Stem-water storage provides an immediate water source to support transpirational demand even when the soil water is abundant, because the long distance between leaves and soil and the associated high hydraulic resistance limit the immediate

This manuscript has been authored by UT-Battelle, LLC under Contract No. DE-AC05-00OR22725 with the US Department of Energy. The United States Government retains and the publisher, by accepting the article for publication, acknowledges that the United States Government retains a non-exclusive, paid-up, irrevocable, world-wide license to publish or reproduce the published form of this manuscript, or allow others to do so, for United States Government purposes. The Department of Energy will provide public access to these results of federally sponsored research in accordance with the DOE Public Access Plan (<http://energy.gov/downloads/doe-public-access-plan>).

use of soil water in tall trees (Zang et al., 1996). In this way, stem-water storage helps minimize the temporal imbalance between water supply and demand and maintain the integrity of water transporting pathway. A diurnal fluctuation of stem-water content and stem diameter has been observed (Goldstein et al., 1998) as a response to the diurnal variation of the two processes, that is, the water extraction from tree stems for transpiration and their replenishment of water from the soil. Though small in size compared with soil water pool, water stored in tree stems provides 6% to over 50% of daily transpiration (Goldstein et al., 1998; Scholz et al., 2008; Köcher et al., 2013; Carrasco et al., 2015) depending on tree species. This contribution was found to increase after drought, for example, from 12% of daily transpiration when soil water is abundant to 25% at the end of summer after a drought period (Loustau et al., 1996). The diurnal storage capacity, that is, as the mass of water that can be withdrawn from the tree stems during the days, has been found to be related to tree allometry, and trees with larger trunks were observed to store and provide more water for plant consumption (Goldstein et al., 1998). Other traits, such as wood density, hydraulic conductivity, or degree of isohydry (as minimum daily branch water potential), can also regulate stem storage and daily water extraction (Meinzer et al., 2003). Seasonally, storing water in trees stems is also one of the plant drought-coping strategies for many species (Borchert, 1994). This is because the internal storage can lower the risk of xylem embolism and consequent hydraulic failure (Hao et al., 2013; Carrasco et al., 2015) by dampening the response of xylem tension to transpiration.

As a key and basic component of the soil–plant–atmosphere continuum and thus regional and global hydrological cycles, plant hydraulics has received growing attention in recent years in the modelling community. Relevant modelling activities have been focused at individual tree scales (e.g., Sperry et al., 1998), ecosystem scales (Williams et al., 2001), and global scales (Bonan et al., 2014; Fisher et al., 2010; Hickler et al., 2006), necessitating a trade-off between complexity and computational cost. Models developed at the individual tree scale can be very detailed as they divide the water flow path into many segments with different hydraulic properties and model three-dimensional water flow. Due to their large spatial coverage, regional and global climate models have to be highly abstract in the treatment of plant hydraulics. Hickler et al. (2006) incorporated the plant hydraulics module into the Lund–Potsdam–Jena Dynamic Global Vegetation Model, Fisher et al. (2010) improved the Community Land Model (CLM) with Ecosystem Demography by adding plant hydraulics, and Bonan et al. (2014) put a similar model into the CLM version 4 (CLM4). They, however, did not explicitly simulate a stem-water storage and its temporal dynamics, which is the focus of this study.

Given the importance of this internal water storage on plant water economics, this research aims to develop an explicit stem-water storage module and associated modelling schemes appropriate for the land component of large-scale Earth system models. We further aim to demonstrate the characteristics of stem-water dynamics and its role in controlling the plant water usage. We will address the following scientific questions: How does the stem-water storage vary diurnally and seasonally? How much does the stem-water storage

contribute to transpiration? Can the inclusion of explicit stem-water storage induce more accurate simulation of Amazon rainforest responses to seasonal drought? The host model used, CLM4, is briefly introduced in Section 2. The parameterization and implementation of a stem-water storage as well as experimental design are also described there. Section 3 presents the results. We then conclude our major findings in Section 4.

2 | METHODOLOGY

We built the stem-water module for the CLM4 (Oleson et al., 2010), the land component of Community Earth System Model version 1.0. CLM4 characterizes hydrological, biophysical, and biochemical processes at scales ranging from plant functional type level to atmospheric grid level. CLM4 assumes that only soil and an underground aquifer store water and the former directly provides water for plant use. The 1D Richards' equation (Equation (1)) governs water transport, with infiltration and subsurface drainage serving as the upper and lower boundary conditions. Only its first layer is responsible for soil evaporation. Plant transpiration is treated as a sink term in the equation and regulated by stomata. Plants physiologically adjust the opening and closing of stomata to regulate their use of water as constrained by soil water availability. A "beta" factor ranging from 0 to 1 is used to describe the soil water availability, derived by considering some limiting values, that is, the levels of soil water when stomata start to close and the wilting point. Transpiration loss is divided between soil layers according to their relative water abundance.

Our "big stem" model treats the tree stems as one virtual stem instead of many individuals separately. Geometric characteristics including basal area, tree height, and stem diameter were used to estimate the size of stem storage and scale stem-water content. The 1D Richards' equation used to describe water diffusion within the soil layers in CLM4 is easily extended to the soil/tree stem system without changing its form,

$$\partial\theta/\partial t = -\partial q/\partial z - s, \quad (1)$$

where θ is the volumetric water content (m^3/m^3) of soil layers or tree stem, s is the sink term for transpiration loss, t is time, z is depth, and q is the flux out of the depth.

The Richards' equation is solved numerically by dividing the soil and stem storage domain into several layers in the vertical direction (10 layers of soil as default in CLM4 and one layer of stem for simplicity) and then integrating downward over each of the model layers. For the i th layer (either soil or stem layer), the change of water amount in unit time equals to the difference of net water flux into the layer and the sink term,

$$\Delta z_i \partial\theta_i/\partial t = -(q_{i,\text{lower}} - q_{i,\text{upper}} - e_i), \quad (2)$$

where $q_{i,\text{lower}}$ and $q_{i,\text{upper}}$ are the water fluxes across the lower and upper boundary of this layer, respectively, and e_i is the sink term. We

define the upward direction as positive for water fluxes. The flux between two elements is given by the Darcy's law,

$$q = -K[\partial(\varphi + z)/\partial z], \quad (3)$$

where K (m/s) and φ (m) are the hydraulic conductivity and water potential of specific elements (soil or tree stem). The soil hydraulic conductivity and water potential depend on mineral composition and abundance of organic matter (e.g., Clapp & Hornberger, 1978).

The soil–plant hydraulic path can be viewed as a series of electric resistors, with its total hydraulic resistance being the sum of all those along the path, namely, the soil-to-root resistance, r_{sr} , and xylem resistance, r_x ,

$$r_{\text{tot}} = r_{sr} + r_x. \quad (4)$$

According to Gardner (1960), the soil-to-root resistance can be estimated by assuming the root system to be a single tube that extracts water from the surrounding soil over a distance,

$$r_{sr} = \log(R_{\text{cyl}}/R_r)/2\pi L_v \Delta z K_s, \quad (5)$$

where K_s is the soil hydraulic conductivity (m/s), R_r is the root radius (m) and is set as 3×10^{-4} m (Manzoni et al., 2013). Although studies have reported the variation of fine root radius with depth (e.g., Maeght et al., 2015), we use a constant value here for simplicity. R_{cyl} (m) is the radius of the soil cylinder to which the root has access to (Newman, 1969),

$$R_{\text{cyl}} = 1/(\pi L_v)^{1/2},$$

where L_v is root length density, which is approximately 1,000 m/m³ for fine roots (radius < 1 mm) in Amazonian soils (Nepstad et al., 1994). Δz is the depth of soil layer (m).

Xylem conductivity is calculated according to the traditional Hagen-Poiseuille equation,

$$r_x = 32\eta S/\pi \sum_{i=1}^n D_i^2, \quad (6)$$

where η is the viscosity of water (1.002 MPa·s at 20°C), S is the length of the xylem tube, which is set as the tree height here, n is the number of vessels, and D is the vessel diameter. Zach et al. (2010) measured trunk vessel diameter and vessel density from 51 trees growing in a lower montane rainforest in Sulawesi, Indonesia. Vessel diameters range from 69.4 to 199.2 μm and vessel density from 2.9 to 16.3 mm^{-2} . Another measurement from 40 Asian tropical trees species reported vessel diameters from 61.8 to 226.2 μm (136.4 $\mu\text{m} \pm 42.2 \mu\text{m}$) and vessel density from 2.2 to 24.2 mm^{-2} (9.1 $\text{mm}^{-2} \pm 6.1 \text{mm}^{-2}$; Fan et al., 2012). On the basis of those measurements, we set D to 130 μm and vessel density to 9 mm^{-2} . The number of vessels, n , is obtained as the vessel density multiplied by sapwood area, with the latter estimated from a species-independent empirical relationship between sapwood

area (cm²) and DBH (diameter at breast height, cm), sapwood area = 1.582 DBH^{1.764} (Meinzer et al., 2001). Here, we use a constant xylem conductivity that is only dependent on uniform vascular anatomy for simplicity. Actual conductivity depends largely on the distribution of cell diameters and is heavily weighted by the largest cells (Tyree & Ewers, 1991). Hydraulic resistance from xylem perforation plates that separate individual vessels can reduce conductivity by up to 18% (Ellerby & Ennos, 1998) and was not considered in this exercise. In addition, variation in conductivity due to water volume or solutes, temperatures, or other factors, for example, the cavitation and refilling processes, are also not considered here.

Water relation curves that directly relate stem-water content to its water potential are seldom reported. Zweifel et al. (Zweifel et al., 2001; Zweifel & Häslar, 2000) developed a sigmoid function to describe their relationship. Their definition requires additional parameters, which makes the equation complex. In this study, we use a similar water relation curve as in soil,

$$\varphi = \varphi_{\text{sat}}(\theta/\theta_{\text{sat}})^{-b}, \quad (7)$$

where φ is the stem-water potential and is set to not exceed -4 MPa following Zweifel et al. (2001). φ_{sat} is the water potential at saturation, set as -100 mm (corresponding to $-1,000$ Pa) and close to the saturation water potential of soil at the specific site in this study in order to maintain the equilibrium of the soil-plant system at saturation. θ is the volumetric water content, and θ_{sat} is the maximum volumetric water content the stem can reach. $\theta/\theta_{\text{sat}}$ is the level of stem saturation. We set the stem-water potential as about -1 MPa when the stem is 50% saturated, giving the constant parameter b of 10.0.

The size of stem-water pool (in volume) is estimated as the tree stem volume multiplied by θ_{sat} . According to Borchert (1994), the saturation water content with respect to dry mass of tree stems is $WC_{\text{sat}} = 100 \cdot \frac{SM-DM}{DM} = 100 \cdot \frac{1-D/1.5}{D}$. SM is the stem mass at saturation, DM is the dry mass, and D is the wood density (g/cm³). The approximate species-independent value is 1.5 g/cm³ for wood density excluding open spaces due to the similar composition of wood: cellulose and lignin (Williamson, 1984). WC_{sat} is the saturation water mass as a percentage of DM and thus can be converted to volumetric water content at saturation, θ_{sat} , as $WC_{\text{sat}} = \theta_{\text{sat}} \cdot \rho_{\text{water}}/D$.

Our study site is the km83 Tapajos national forest in central Amazonia (3.0180°S, 54.9714°W). It is mainly covered by evergreen broadleaf rainforest with 35-m canopy height. A mean DBH measured at this study site is 1.02 m (Figueira et al., 2011). The basal area was measured at three plots near the flux tower in the Tapajos forest (3.31°S, 54.94°W) in 1995 as 26.89, 31.31, and 34.39 m²/ha (Baker et al., 2004). Baker et al. (2004) measured the wood density near the BR-Sa3 site with the average value among different methods and plots of 0.65 g/cm³. θ_{sat} was thus obtained as 56.67% for this site. The average daily precipitation at this site is 12 mm. The dry season with daily rainfall lower than 2 mm is from August to October. A tower mounted with measurement equipment was set up at this site. Measurements that include meteorological variables (e.g., wind speed, air temperature, air humidity, air pressure precipitation, incoming solar

and thermal radiation, and outgoing solar and thermal radiation), surface energy fluxes (e.g., sensible and latent heat fluxes), and environmental variables (e.g., soil moisture) were taken at a half hourly time scale from 2000 to 2004. The precipitation measurement at the K83 site might be underestimated because it is 15% lower than that given by the Global Precipitation Climatology Product during 2001–2003 (Adler et al., 2003). A comparison of the precipitation at the K83 site with that of the other two adjacent evergreen rainforest sites (K67 and k77) revealed an obvious low wet-season precipitation at K83 site. To fix this underestimation, we increased the rainy season rainfall by 15% following Yan and Dickinson (2014).

Our ability to directly validate those simulation results is limited by both spatially and temporally sparse observations of stem-water dynamics, as well as the lack of the accompanying meteorological and physiological variables. Instead, we attempted to at least show that the basic characteristics of stem-water dynamics were captured by the updated model. To demonstrate the differences caused by the inclusion of stem-water storage, we conducted two numerical experiments, one with stem-water storage (EXP) and one without (CTL), with both versions taking into account the root and stem resistance to water flow. We ran offline CLM4 simulations using the prescribed satellite phenology at the K83 site forced by the site measured meteorological variables. Gaps of measurement due to interruption of precipitation or equipment malfunction were filled by linear interpolation. The leaf area index and soil texture at this site were extracted from the default global gridded dataset provided by CLM4. The plant functional type was set to be evergreen broadleaf forest, and its coverage was set to be 100%. The simulation was from September 2001 to December 2004, and the time step was half hour. CLM4 checked water balance at each time step to ensure that water balance error was not higher than a threshold (10^{-7} mm). For both sets of CLM experiments, water balance was routinely checked. The water balance error was far less than the threshold with mean value of 1.01×10^{-12} mm and maximum value of 2.95×10^{-10} mm.

3 | RESULTS

3.1 | Seasonal variations

As shown in Figure 1a, the year 2002 had a pronounced dry season from August to October with very low precipitation. Though several strong precipitation events occurred in November and December, the period of most continuously high precipitation (characteristics of the wet season) did not return until the next January. In contrast, in 2003, it rained moderately from August to October, the climatologically dry season at this location, leading to a lack of a well-developed dry season for this year. Hence, the analysis for dry season below is focused on year 2002.

These two experiments were in good agreement for the daily mean latent and sensible heat flux when there was no water stress (Figure 1b,c). The major discrepancy occurred during the 2001 and 2002 dry seasons, where the default model

underestimated/overestimated latent/sensible heat flux due to an underestimation of water availability, a well-known deficiency in CLM4 over the Amazon rainforest region (Lee et al., 2005; Zheng & Wang, 2007). EXP improved this deficient drought response in the 2002 dry season, with good agreement with observations (OBS), but overestimated latent heat flux in the less pronounced 2001 dry season.

The saturation level of tree stems exhibited a pronounced seasonal variation following the pattern of precipitation (Figure 1d), higher in the wet season than in the dry season, indicating that water storage inside tree stems was used to support dry-season transpiration. The stem-water amount fluctuated pronouncedly at the beginning of the wet season, became more stable for the rest of the wet season, and then decreased gradually during the dry season in response to the loss of stem-water to transpiration (Figure 1e). Stem-water contributed around 45% of daily transpiration during the wet season, and the proportion went up during the dry season reaching up to 70%. As shown in Figure 2, daytime sap flow peaked in the wet season, but nighttime sap flow peaked in the dry season. The lag between the two peaks was also seen in field observations (e.g., Wang et al., 2011).

3.2 | Diurnal cycles

EXP and CTL coincided with each other in terms of latent/sensible heat fluxes in the wet season and agreed very well with observations (Figure 3a). In contrast, dry-season latent heat flux from EXP exceeded that from CTL for all the three months, associated with lower sensible heat flux from EXP than that from CTL, with EXP closer to OBS (Figure 3b). In the 3-month dry season of 2002, latent/sensible heat flux from CTL was significantly higher/lower than that from observations with p values of $9.456e-05$ (latent) and $1.482e-13$ (sensible). The p values between EXP and observations was much higher for both latent (.006934) and sensible (.02663) heat fluxes. A comparison of daily maximum values of the two turbulent energy fluxes between simulations and observations in Figures S1 and S2 also supported that the experimental model was much closer to observations.

The diurnal pattern of stem saturation (Figure 4) featured three periods: (a) Stem-water content decreased during 6:30 am–2 pm to support transpiration; (b) increased during 2 pm–midnight in response to the recharging of stem-water storage by soil water; and (c) continued to increase from midnight to 6:30 am with a lower rate of increase. The major difference between the three months lay in the strength of the refilling processes after midnight, which increased from August to October (not shown). Through the dry season, the magnitude of diurnal fluctuation in stem saturation increased, that is, was more pronounced, when water stress was more severe.

The canopy sap flow is defined as the sap flow across the top boundary of the stem pool, that is, very close to the canopy, and is equal to the transpiration rate. Basal sap flow is the accumulated sap flow from each soil layer to the stem-water storage. Canopy sap flow

FIGURE 1 Daily averaged model simulations and observations at the BR-Sa3 site during September 2001 to February 2004: (a) observed precipitation (mm); (b) a comparison of sensible heat flux among model simulations from CTL (blue), EXP (red), and observations (black); (c) the same as (b) but for latent heat flux; (d) the percentage of stem saturation; and (e) stem-water contribution to transpiration

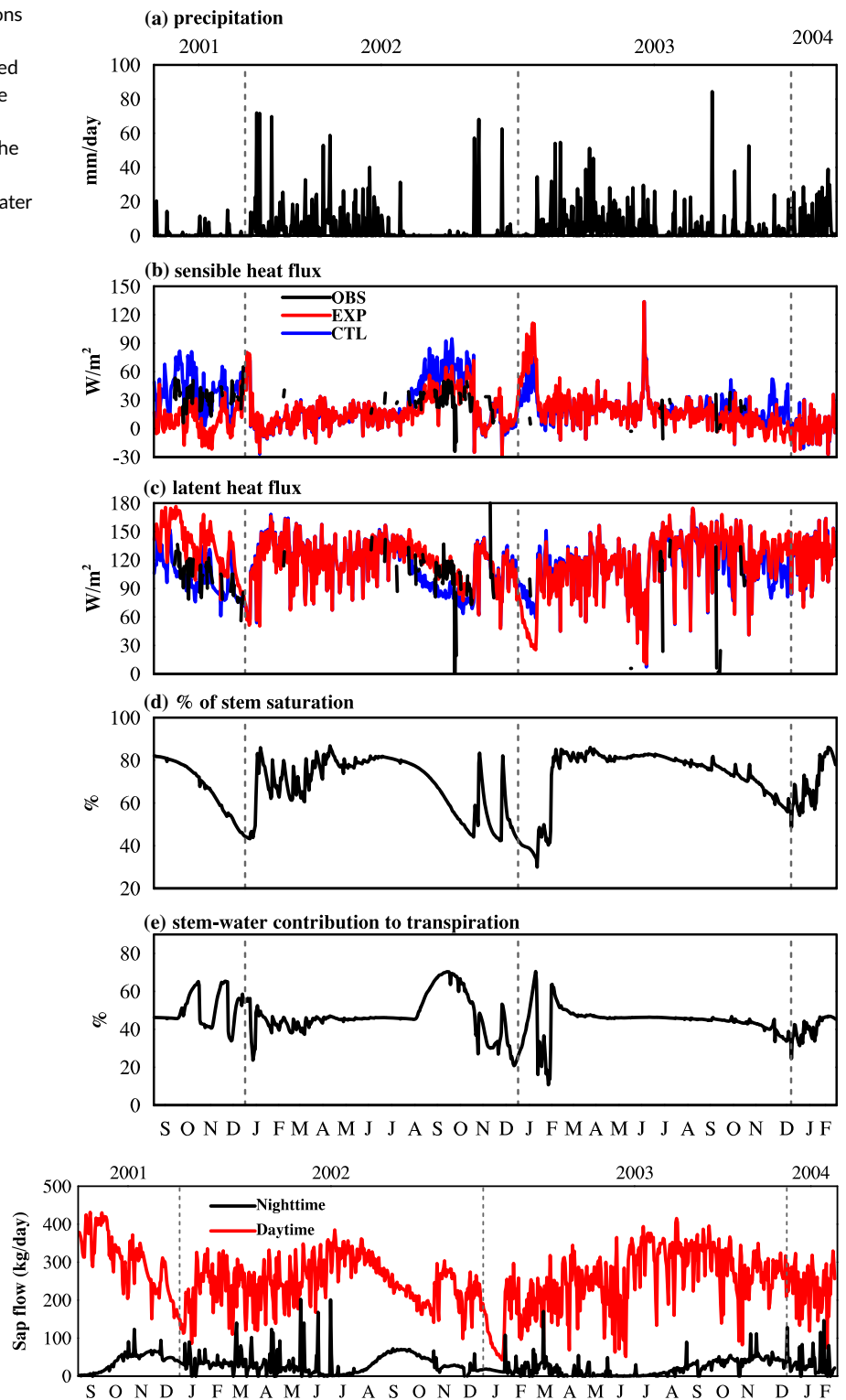


FIGURE 2 Daytime and nighttime sap flow rate for a single tree

was zero at night, corresponding to the assumption in the CLM that plants stop transpiration during the night. It increased in the morning with the onset of transpiration and reached its peak around 11 am–12 pm. It remained at its peak value for about 3–5 hr and then started to decrease in the afternoon. Basal sap flow generally followed the diurnal pattern of canopy sap flow except that nighttime sap flow was positive, indicating nighttime refilling of stem-water storage by soil water. The growth of basal sap flow starting at sunrise was weaker

than its canopy counterpart. It reached its peak around 2 pm–3 pm, about 3 hr later than the peak of canopy sap flow.

The time lag between sap flow at these two elevations increased from early to late dry season. The hysteresis of the two sap flows was demonstrated in Figures 5, S3, and S4. Basal sap flow decreased from the late afternoon to the night and then decreased more gradually in the night. The magnitude of basal sap flow was generally lower than that of canopy sap flow during most of the daytime. Its peak value

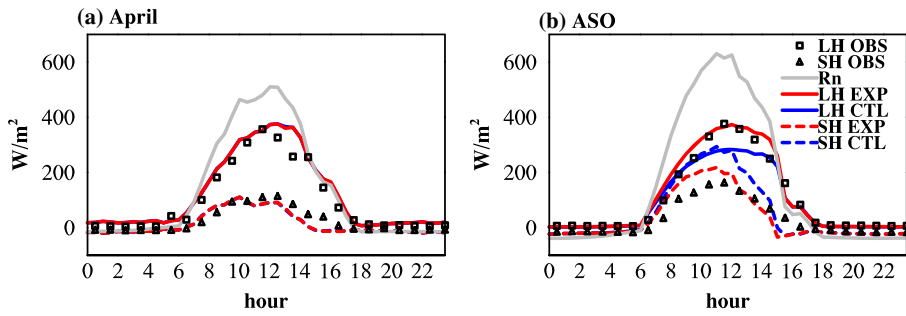


FIGURE 3 Seasonally averaged diurnal cycles of net radiation (Rn), sensible heat flux (SH), and latent heat flux (LH) in (a) wet season (April) and (b) dry season (August, September, and October) of 2002

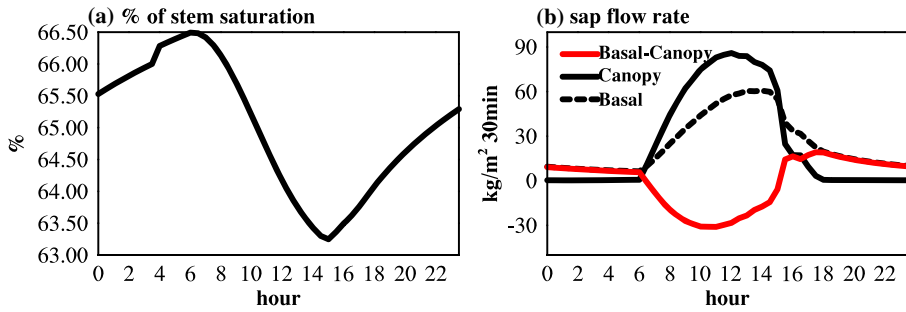


FIGURE 4 Diurnal cycle of (a) stem-water content and (b) sap flow rates from EXP averaged through the dry season of 2002

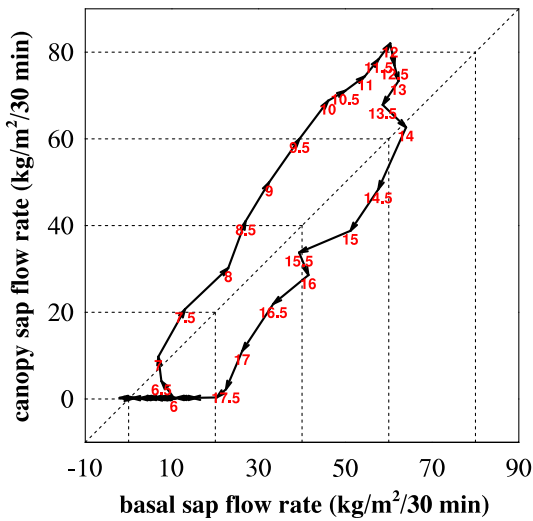


FIGURE 5 The onset and magnitude of the hysteresis between basal and canopy sap flows in August 2002. Values in the figure are monthly mean. Red numbers indicate the hour of the day

decreased from early to late dry season, indicating decreasing ability of soil water to recharge stem-water storage. Its peak value was about $90 kg/m^2/30 min$ (August), $50 kg/m^2/30 min$ (September), and $40 kg/m^2/30 min$ (October), corresponding to 40, 22.9, and 18.28 kg/hr per single tree after being scaled by the allometric parameters.

The simulated net change of stem-water content was illustrated in Figure 4b by the difference between basal and canopy sap flow rates. Positive value means higher basal sap flow rate and lower canopy rate and hence indicates a net recharging process. On the other hand, a negative value represents a net discharging process. Most of the daytime was dominated by a net discharging process, whereas the late afternoon and nighttime were dominated by a net recharging process.

3.3 | Seasonal evolutions in diurnal cycles of stem-water content

Though sharing similar diurnal patterns over the year, the simulated stem-water amount had large seasonal variations (Figure 6a),

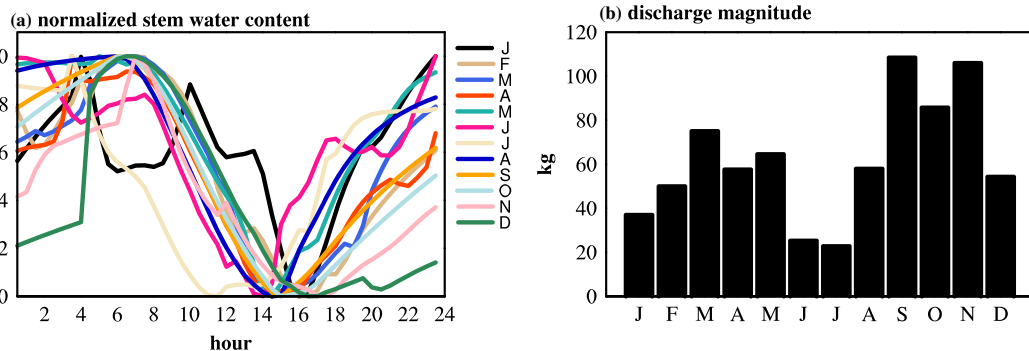


FIGURE 6 The seasonal evolution of diurnal cycles of (a) the normalized stem-water amount and (b) the daily discharge magnitude of a single tree

especially in the timing of the transition from net discharging to net recharging in the afternoon as well as the recharging strength from midnight to the early morning. Stem-water amount peaked at about 6 am after the whole night of refilling by the soil water and reached its minimum in the afternoon due to its support of transpiration. The difference between the peak and the minimum water amount inside the stem, defined as discharge magnitude here, thus can serve as a proxy for the stem contribution to transpiration per day. Figure 6b showed that this contribution was higher in the dry season than in the wet season, consistent with Figure 1e. The discharge magnitude was

about 20–80 kg/day in the wet season and about 90–110 kg/day in the dry season.

3.4 | The dynamic nature in sap flows: Cloudy versus sunny days

The recharging/discharging processes were dynamic in response to environmental conditions (Figure 7). The relative strength of the two processes hence determined the dynamic variability of stem-water content. Higher peak of net radiation at noon in the cloudy day than in the sunny day was likely owing to the higher longwave forcing under cloudy conditions, compared with clear sky (Figure 7a). The diurnal evolution of sap flow was quite smooth on the sunny day, whereas it fluctuated considerably on the cloudy day. The canopy sap flow also dropped to and stayed at zero for a period of time during the afternoon before it peaked again later (Figure 7b). As a result, the stem recharge was quite pronounced during that period, leading to a weaker recharge rate at night than on a sunny day (Figure 7c).

4 | CONCLUSIONS AND DISCUSSION

Widespread tree mortality as a result of drought and heat stress have been observed over the globe, especially over tropical areas (Allen et al., 2010). A recent model intercomparison, however, reveals large discrepancies in modelling these vegetation dynamics and carbon cycles in response to droughts (Powell et al., 2013), especially for tropical forests (Sitch et al., 2008). For example, the current generation of models was found to be deficient in capturing the correct response of tropical forests to water stress or drought. This widely known bias in their underestimation of dry-season evapotranspiration rates was mainly attributed to the lack of key and necessary hydraulic components and processes in the modeled vegetation–soil system (Zheng & Wang, 2007). Xu et al. (2013) thus commented that “increased efforts to improve our current understanding of ecosystem responses to water stress are urgently required.”

The internal water pool inside tree stems plays a key role in plant water economics especially for Amazonian tropical trees with large stems. We developed a stem-water storage module and incorporated it into CLM4, the land surface component of Community Earth System Model 1.0. Stem-water dynamics and its contribution to daily transpiration were simulated at one eddy covariance site in the central Amazonia, BR-Sa3. The study site is dominant by evergreen broadleaf trees and experienced a dry season of 3 months from August to October with mean daily precipitation lower than 2 mm. On the seasonal time scale, stem-water amount followed that of precipitation, that is, higher in the wet season than in the dry season. As the dry season started, the stem-water content decreased to support transpiration. The contribution of stem-water to daily transpiration was around 45% in the wet season and can reach up to 70% in the dry season at this site. The greater contribution from stem-water in the dry season was

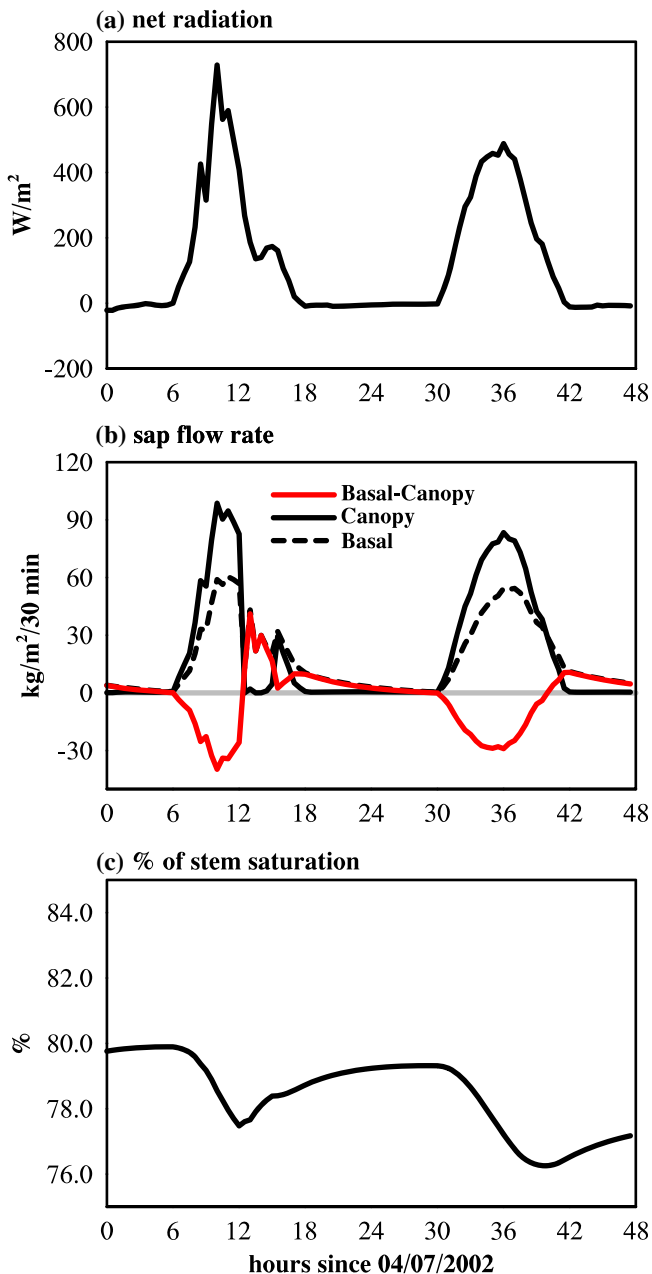


FIGURE 7 A comparison of (a) net radiation, (b) sap flow rate, and (c) stem saturation percentage from two consecutive dates with first cloudy and second sunny indicates the dynamic nature of discharge and recharge processes

consistent with field observations (Wang et al., 2011), but its magnitude was greater than reported values from other sites: 9%–15% in tropical trees in Panama (Goldstein et al., 1998), 6%–28% in subtropical trees (Carrasco et al. 2015), and up to 50% in conifers (Lostau, 1996; Waring et al., 1979). Another stem storage model, parameterized with sap flow measurements in *Picea*, indicated variation in use of stored water from 1%–44% of daily transpiration (Verbeek et al. 2007). Using theoretical hydraulic conductivity with a single vessel diameter and perfectly circular cell is likely to overestimate actual conductivities by up to five times (Tyree & Ewers, 1991), and our results should be considered in context of that uncertainty. Moreover, those aforementioned observations were reported at locations other than our site and for species sometimes different from the dominant species at the site we used, leading to potential discrepancies in the contribution percentages from our simulations.

The diurnal cycle of stem-water amount is produced by two competing processes, recharging and discharging, which are determined by the relative strength of canopy and basal sap flow rate. Canopy sap flow provides evidence of water flux that directly feeds transpiration, whereas the basal sap flow indicates replacement of canopy xylem water and refilling of storage pools. During the three months in 2002 dry season, the peak value of basal sap flow rate was about 90 kg/m²/30 min (August), 50 kg/m²/30 min (September), and 40 kg/m²/30 min (October), corresponding to 40, 22.9, and 18.28 kg/hr per single tree after being scaled by the allometric parameters, similar to the 50 kg/hr measured in a similarly sized 1-m diameter tropical tree in Panama (Goldstein et al., 1998). Another measurement by Gilbert et al. (2006) reported basal sap flow rate for a large, diffuse-porous *Populus nigra* individual at about 25–50 kg/m²/30 min, similar to our simulation results.

The discharge magnitude, defined as the difference between daily maximum and minimum stem-water content, corresponds to the diurnal water storage in other studies (e.g., Goldstein et al., 1998) and was estimated to be higher in the dry season (90–110 kg/day) than in the wet season (20–80 kg/day). This magnitude was greater than the 54 kg/day measured by Goldstein et al. (1998) for a similarly sized tree. The values by Goldstein et al. (1998), however, were derived during an extremely wet period with the total precipitation about 250% above normal and thus due to high water availability and low demand would be expected to be smaller than during drier periods.

The current modelling scheme for soil-to-plant water transfer is quite simplified, leaving many important aspects out of consideration. For example, the xylem that functions to store and transport water within plant bodies can influence water transporting efficiency by varying resistance dependent on water abundance inside the tube (Ayup et al., 2012). In the current parameterization scheme, however, only the water-storing function of xylem is taken into account. Also, a constant instead of variable hydrologic resistance was applied and mainly based on idealized geometric characteristics of the xylem tube. Therefore, further improvement of the basic parameterization scheme towards a more sophisticated and realistic representation of structure,

resistance, and diurnal driving forces associated with water storage is a crucial future challenge.

Extending to a larger spatial scale is another key future challenge. One difficulty for extending the stem pool model to the whole basin scale is the collection of spatially varying and species-specific plant traits (e.g., tree density, diameter, height, xylem wood density, isohydry, and root distribution) over large spatial scales. Possible solutions include employment of some empirical relationships, linking stem diameter and height with the latter gained from remote sensing techniques. The problem may also be solved by performing a large number of simulations and statistical analysis of the simulated results using parameters that span the domain of known capacitance. At the individual tree level, plant hydraulic modelling is well established with most relevant mechanistic processes included. However, plant hydraulics in global models is still very simplified and needs more efforts, in terms of what abstract level is sufficiently accurate and what parameters and parameterizations are optimal. This study can contribute to our understandings in this aspect.

ACKNOWLEDGEMENTS

This work is supported by the Next Generation Ecosystem Experiments-Tropics project and the Terrestrial Ecosystem Science Scientific Focus Area project funded through the Terrestrial Ecosystem Science Program in the Climate and Environmental Sciences Division (CESD) of the Biological and Environmental Research (BER) Program in the U.S. Department of Energy, Office of Science. Oak Ridge National Laboratory is supported by the Office of Science of the US Department of Energy under Contract DE-AC05-00OR22725.

ORCID

Jiafu Mao  <https://orcid.org/0000-0002-2050-7373>

REFERENCES

- Adler, R. F., et al. (2003). The version-2 global precipitation climatology project (GPCP) monthly precipitation analysis (1979–present). *Journal of Hydrometeorology*, 4(6), 1147–1167.
- Allen, C. D., et al. (2010). A global overview of drought and heat-induced tree mortality reveals emerging climate change risks for forests. *Forest Ecology and Management*, 259(4), 660–684.
- Ayup, M., et al. (2012). Changes of xylem hydraulic efficiency and native embolism of *Tamarix ramosissima* Ledeb. seedlings under different drought stress conditions and after rewatering. *South African Journal of Botany*, 78, 75–82.
- Baker, T. R., et al. (2004). Variation in wood density determines spatial patterns in Amazonian forest biomass. *Global Change Biology*, 10(5), 545–562.
- Bonan, G., et al. (2014). Modeling stomatal conductance in the earth system: Linking leaf water-use efficiency and water transport along the soil–plant–atmosphere continuum. *Geoscientific Model Development*, 7(5), 2193–2222.
- Borchert, R. (1994). Soil and stem-water storage determine phenology and distribution of tropical dry forest trees. *Ecology*, 75(5), 1437–1449.
- Chapotin, S. M., et al. (2006). Baobab trees (*Adansonia*) in Madagascar use stored water to flush new leaves but not to support stomatal opening before the rainy season. *New Phytologist*, 169(3), 549–559.
- Clapp, R. B., & Hornberger, G. M. (1978). Empirical equations for some soil hydraulic properties. *Water Resources Research*, 14(4), 601–604.

- Ellerby, D., & Ennos, A. (1998). Resistances to fluid flow of model xylem vessels with simple and scalariform perforation plates. *Journal of Experimental Botany*, 49(323), 979–985.
- Fan, Z. X., et al. (2012). Hydraulic conductivity traits predict growth rates and adult stature of 40 Asian tropical tree species better than wood density. *Journal of Ecology*, 100(3), 732–741.
- Figueira, A. et al., 2011. LBA-ECO CD-04 Dendrometry, km 83 Tower Site, Tapajos National Forest, Brazil, Data set.
- Fisher, R., et al. (2010). Assessing uncertainties in a second-generation dynamic vegetation model caused by ecological scale limitations. *New Phytologist*, 187(3), 666–681.
- Gardner, W.R. (1960). Dynamic aspects of soil-water availability to plants. *Soil Sci.*, 89, 63–73.
- Goldstein, G., et al. (1998). Stem-water storage and diurnal patterns of water use in tropical forest canopy trees. *Plant, Cell & Environment*, 21(4), 397–406.
- Hao, G. Y., et al. (2013). Investigating xylem embolism formation, refilling and water storage in tree trunks using frequency domain reflectometry. *Journal of Experimental Botany*, 64(8), 2321–2332.
- Hickler, T., et al. (2006). Implementing plant hydraulic architecture within the LPJ Dynamic Global Vegetation Model. *Global Ecology and Biogeography*, 15(6), 567–577.
- Huang, C. et al., 2015. The role of plant water storage on water fluxes within the coupled soil–plant–atmosphere system, AGU Fall Meeting Abstracts.
- Huang, C-W, Domec, J-C, Ward, EJ, Duman, T, Manoli, G, Parolari, AJ, & Katul, GG. (2017). The effect of plant water storage on water fluxes within the coupled soil-plant system. *New Phytologist*, 213, 1093–1106.
- Köcher, P., et al. (2013). Stem-water storage in five coexisting temperate broad-leaved tree species: Significance, temporal dynamics and dependence on tree functional traits. *Tree physiology*, 33(8), 817–832.
- Lee, J. E., et al. (2005). Root functioning modifies seasonal climate. *Proceedings of the National Academy of Sciences of the United States of America*, 102(49), 17576–17581.
- Loustau, D., et al. (1996). Transpiration of a 64-year-old maritime pine stand in Portugal. *Oecologia*, 107(1), 33–42.
- Maeght, J. L., et al. (2015). Seasonal patterns of fine root production and turnover in a mature rubber tree (*Hevea brasiliensis* Müll. Arg.) stand-differentiation with soil depth and implications for soil carbon stocks. *Frontiers in Plant Science*, 6, 1022.
- Manzoni, S., et al. (2013). Biological constraints on water transport in the soil–plant–atmosphere system. *Advances in Water Resources*, 51, 292–304.
- Meinzer, F., et al. (2001). Regulation of water flux through tropical forest canopy trees: Do universal rules apply? *Tree Physiology*, 21(1), 19–26.
- Meinzer, F. C. (2002). Co-ordination of vapour and liquid phase water transport properties in plants. *Plant, Cell & Environment*, 25(2), 265–274.
- Meinzer, F. C., et al. (2003). Whole-tree water transport scales with sapwood capacitance in tropical forest canopy trees. *Plant, Cell & Environment*, 26(7), 1147–1155.
- Nepstad, D. C., et al. (1994). The role of deep roots in the hydrological and carbon cycles of Amazonian forests and pastures. *Nature*, 372(6507), 666–669.
- Newman, E. (1969). Resistance to water flow in soil and plant. I. Soil resistance in relation to amounts of root: Theoretical estimates. *Journal of Applied Ecology*, 1–12.
- Oleson, K.W. et al., 2010. Technical description of version 4.0 of the Community Land Model (CLM).
- Powell, T. L., et al. (2013). Confronting model predictions of carbon fluxes with measurements of Amazon forests subjected to experimental drought. *New Phytologist*, 200(2), 350–365.
- Scholz, F. C., et al. (2008). Temporal dynamics of stem expansion and contraction in savanna trees: Withdrawal and recharge of stored water. *Tree Physiology*, 28(3), 469–480.
- Sitch, S., et al. (2008). Evaluation of the terrestrial carbon cycle, future plant geography and climate–carbon cycle feedbacks using five Dynamic Global Vegetation Models (DGVMs). *Global Change Biology*, 14(9), 2015–2039.
- Sperry, J., et al. (1998). Limitation of plant water use by rhizosphere and xylem conductance: Results from a model. *Plant, Cell & Environment*, 21(4), 347–359.
- Tyree, M. T., & Ewers, F. W. (1991). The hydraulic architecture of trees and other woody plants. *New Phytologist*, 119(3), 345–360.
- Wang, H., et al. (2011). Nighttime sap flow of *Acacia mangium* and its implications for nighttime transpiration and stem water storage. *Journal of Plant Ecology*, 5(3), 294–304.
- Waring, R., et al. (1979). The contribution of stored water to transpiration in Scots pine. *Plant, Cell & Environment*, 2(4), 309–317.
- Williams, M., et al. (2001). Use of a simulation model and ecosystem flux data to examine carbon–water interactions in ponderosa pine. *Tree Physiology*, 21(5), 287–298.
- Williamson, G. B. (1984). Gradients in wood specific gravity of trees. *Bulletin of the Torrey Botanical Club*, 51–55.
- Xu, C., et al. (2013). Our limited ability to predict vegetation dynamics under water stress. *New Phytologist*, 200(2), 298–300.
- Yan, B., & Dickinson, R. E. (2014). Modeling hydraulic redistribution and ecosystem response to droughts over the Amazon basin using Community Land Model 4.0 (CLM4). *Journal of Geophysical Research: Biogeosciences*, 119(11), 2130–2143.
- Zach, A., et al. (2010). Vessel diameter and xylem hydraulic conductivity increase with tree height in tropical rainforest trees in Sulawesi, Indonesia. *Flora-Morphology, Distribution, Functional Ecology of Plants*, 205(8), 506–512.
- Zang, D., et al. (1996). Variation of sapflow velocity in *Eucalyptus globulus* with position in sapwood and use of a correction coefficient. *Tree Physiology*, 16(8), 697–703.
- Zheng, Z., & Wang, G. (2007). Modeling the dynamic root water uptake and its hydrological impact at the Reserva Jaru site in Amazonia. *Journal of Geophysical Research: Biogeosciences*, 112(G4).
- Zweifel, R., & Häslner, R. (2000). Stem radius changes and their relation to stored water in stems of young Norway spruce trees. *Trees*, 15(1), 50–57.
- Zweifel, R., et al. (2001). Link between diurnal stem radius changes and tree water relations. *Tree Physiology*, 21(12-13), 869–877.

SUPPORTING INFORMATION

Additional supporting information may be found online in the Supporting Information section at the end of this article.

How to cite this article: Yan B, Mao J, Dickinson RE, et al. Modelling tree stem-water dynamics over an Amazonian rainforest. *Ecohydrology*. 2020;13:e2180. <https://doi.org/10.1002/eco.2180>